Quantum Electronics **40** (11) 942 – 954 (2010)

PACS numbers: 81.07.–b; 81.16.–c; 81.16.Rf
DOI: 10.1070/QE2010v040n11ABEH014447

Laser nanostructuring of materials surfaces

I.N. Zavestovskaya

Abstract. **This paper reviews results of experimental and theoretical studies of surface micro- and nanostructuring of metals and other materials irradiated directly by short and ultrashort laser pulses. Special attention is paid to direct laser action involving melting of the material (with or without ablation), followed by ultrarapid surface solidification, which is an effective approach to producing surface nanostructures. Theoretical analysis of recrystallisation kinetics after irradiation by ultrashort laser pulses makes it possible to determine the volume fraction of crystallised phase and the average size of forming crystalline structures as functions of laser treatment regime and thermodynamic properties of the material. The present results can be used to optimise pulsed laser treatment regime in order to ensure control nanostructuring of metal surfaces.**

Keywords: *nanostructures, short and ultrashort laser pulses, laser ablation, rapid solidification.*

1. Introduction

Laser micro- and nanostructuring of materials is important in many scientific, technological and medical applications, such as the fabrication of opto- and nanoelectronic devices, information storage systems, control over the mechanical and optical properties of solids and biomedical engineering [1 – 8]. Nanostructures resulting from laser material processing have unique properties and often cannot be produced by other, nonlaser techniques.

The production of nanoscale structures on the surface of solids improves their physical and mechanical properties, enhances the biocompatibility of implants with body tissues, etc. For example, the strength of structural materials increases with decreasing grain size, with no loss in plasticity [9]. Nanostructured materials strongly differ in optical properties from unmodified bulk materials, acquiring properties of metamaterials. This can be used to increase the absorptance of materials by laser processing [10, 11], to produce black and coloured films on the surface of various metals [11 – 15] and to fabricate 'black silicon' structures [7, 16] for solar-cell manufacturing. In addition, nanostructured surfaces find application in selective nanocatalysis, microelectronics for information recording, processes for creating optical memory based on phase transitions in metal nanoparticles etc. [17].

Laser micro- and nanostructuring processes take advantage of physical mechanisms that underlie the formation of two- and three-dimensional micron- and nanometre-scale structures in metals, semiconductors, transparent materials, and polymers illuminated by laser pulses of various intensities and durations.

The development of laser nanostructuring technologies has been stimulated by recent advances in laser engineering, which have made it possible to generate short and ultrashort laser pulses. Considerable effort has been aimed at improving the performance and lowering the cost of femtosecond laser systems, which have proved effective in a variety of applications [13 – 23]. Moreover, recent years have seen increasing use of diode-pumped solid-state lasers generating nanosecond pulses [24 – 26]. Such lasers offer the advantages of small dimensions, good beam quality and high efficiency.

Nanostructuring with short and ultrashort laser pulses is possible under various laser ablation conditions and also under subthreshold conditions that ensure rapid melting of the surface layer.

Issues pertaining to laser – matter interactions, in particular, laser ablation mechanisms, have been addressed in many reports (see e.g. Refs [1, 27 – 32] and references therein). Intense, detailed research into the physics of laser – matter interactions was probably triggered by the idea put forward by Basov and Krokhin [33] as early as more than forty years ago that lasers could be used to achieve controlled fusion. The fundamental works by Afanasiev and Krokhin [34 – 36] presented a physical picture of processes initiated in solids by nanosecond laser pulses of various intensities. Later, using theoretical analysis and numerical modelling, Afanasiev et al. [37 – 43] explored various aspects of metal and polymer ablation with ultrashort (pico- and femtosecond) laser pulses.

The energy of a laser pulse is first absorbed in the affected zone and then transferred to the bulk of the material and its lattice through heat conduction processes due to electron – phonon coupling. Mechanisms of laser radiation absorption by electrons may be both linear and nonlinear. Nonlinear light absorption at high incident laser intensities has been extensively discussed in the literature

I.N. Zavestovskaya P.N. Lebedev Physics Institute, Russian Academy of Sciences, Leninsky prosp. 53, 119991 Moscow, Russia;
e-mail: zavest@sci.lebedev.ru

Received 25 August 2010; revision received 6 October 2010
Kvantovaya Elektronika **40** (11) 942 – 954 (2010)
Translated by O.M. Tsarev

because it determines the effect of ultrashort laser exposure on transparent materials such as wide-gap semiconductors and dielectrics [44–47]. Ultrashort laser pulses rapidly heat the electronic system to temperatures in the order of tens of thousands of kelvins, whereas the lattice remains at room temperature. The key features of the electron thermalisation kinetics in such a system, energy transfer from the electrons to the lattice and the timescales of these processes have been analysed in a number of publications [1, 42]. Energy transfer from electrons to lattice phonons takes several picoseconds. The heated region then acts as the source of a thermal wave which propagates to the bulk of the material (heat conduction processes in metals exposed to femtosecond pulses under nonequilibrium conditions were examined by Kanavin and Uryupin [48, 49]). Thus, the absorbed laser pulse energy acts as a surface heat source.

Sufficiently high incident laser intensities may cause structural and phase changes, such as melting; vaporisation, possibly accompanied by laser plasma generation; and ablation, involving the ejection of surface atoms or particles of the material [1, 28–31, 50–56]. The structural and phase changes may lead to surface nanostructuring and nanoparticle formation away from the material surface. It has long been known that, under certain conditions, laser-induced material ejection from an exposed surface region may lead to the formation of various micron- and nanometre-scale periodic structures in the affected zone [11, 31, 57–61]. Moreover, laser-induced surface material removal leads to the formation of nanoclusters [3, 7, 8, 22, 62–64], which may then redeposit on a substrate, leading to the formation of a nanostructured surface film [65]. Nanocluster formation is possible both in the ablation regime, where laser plasma effects are minimal, and with direct participation of a laser plasma [3, 7, 64]. Cluster formation in a liquid may yield a suspension of nanoparticles widely used in biomedical applications [3, 7, 12, 66, 67].

In recent years, a great deal of attention has been paid to the possibility of so-called direct surface nanostructuring with ultrashort laser pulses, where structures are formed at specific laser radiation parameters [8, 22, 53, 63, 68]. Direct surface nanostructuring means that nanoscale surface structures are produced without redeposition of ejected particles onto specially prepared substrates, without any screening masks, etc. Nanostructuring is only caused by a laser beam incident directly on the surface of bulk material or film. One can use repetitive-pulse exposures. The size of forming nanostructures can be controlled by varying the number of pulses [61]. A distinctive feature of direct laser nanostructuring is that the processes involved are inherent in laser ablation, which involves melting and/or material ejection in the form of atoms, followed by redeposition of the atoms and/or clustering in the vapour phase. In the case of melting, surface nanostructuring is governed by the surface cooling rate after the laser pulse.

Direct laser micro- and nanostructuring of material surfaces is receiving increasing attention because this method is simple and cheap [5, 60, 63, 68]. It ensures both locality of the action and the possibility of large-area processing using programmable beam scanning. An important practical issue is then the ability to control and reproduce laser nanostructuring processes.

Ultrashort laser pulses may cause ablation without melting the material. In surface processing with femtosecond laser pulses, the ablated material may have high energy (in the vapour phase), which essentially rules out its redeposition onto the surface (especially in the form of microdroplets). As a result, only the material in the zone under laser irradiation is heated and ejected. The irradiated area undergoes morphological changes and nanostructuring [19, 69, 70].

If there is a liquid material, it rapidly solidifies by virtue of the heat transfer to the interior of the sample after the laser pulse. Because of the very high cooling rate (10^7 K s^{-1} or above), the size of the forming crystallites may be comparable to interatomic distances [26, 30, 56, 71]. This causes structural changes in the irradiated zone, including effective nanostructuring of the solidified material. If the cooling rate exceeds the crystallisation rate, an amorphous layer may form [25, 26, 72].

In optimising laser nanostructuring conditions, an important point is to minimise the size of the resulting structures. The minimum possible size of the structures (holes, etch pits) produced by direct laser ablation of the surface in the material ejection regime is determined by the diffraction-limited beam divergence and is comparable to the laser wavelength [18–20]. When $\sim$ 800-nm titanium:sapphire laser pulses are used in surface processing, only micron-scale structures can be produced by direct ablation. Ablation with femtosecond laser pulses can produce submicron-scale structures only when the laser beam is carefully focused [20, 53]. High-quality structures can then be obtained, up to 100 nm in resolution or depth. The minimum possible size of such structures is limited by the stability and quality of the femtosecond laser beam intensity profile. Surface structures tens of nanometres in size can be produced by the above indirect laser treatment methods through redeposition of forming nanoparticles onto substrates and by near-field ablation, e.g. using a femtosecond laser pulse in combination with scanning microscopy or atomic force microscopy [3, 5–7].

Direct laser irradiation can produce very small structures (tens of nanometres in size) on the surface of materials in two instances: (1) intense laser ablation due to cluster redeposition in and outside the ablation crater and (2) ultrashort laser pulses which ensure very rapid heating, melting and solidification of metal surfaces. Laser structuring without ablation is possible when the pulse energy density is slightly below the ablation threshold but exceeds the melting threshold. Use is typically made of short and ultrashort (nano-, pico- and femtosecond) laser pulses with near-threshold intensities, which cause local metal melting with no significant ablation.

In recent years, controlled direct surface nanostructuring with laser pulses under such conditions has been the subject of intense research. Attempts were made to systematically study laser nanostructuring mechanisms and optimise processing conditions (intensity, duration, number and repetition rate of laser pulses) with consideration for the thermodynamic characteristics, mechanical properties and surface quality of the target material [10, 22, 26, 68].

This paper reviews the results of experimental and theoretical studies of micro- and nanomodification processes induced on the surface of metals and other materials by short and ultrashort laser pulses, with focus on the results obtained by researchers at the N.G. Basov Quantum Radiophysics Division, P.N. Lebedev Physics Institute, Russian Academy of Sciences. Particular attention will be

paid to the possibility of direct laser nanostructuring through melting of the material (with or without ablation), followed by ultrarapid solidification of the molten surface layer, resulting in the formation of nanoscale surface structures.

2. Direct laser nanostructuring of materials surfaces: experimental results

Direct laser micro- and nanostructuring (modification) of materials surfaces involves both producing a fine-crystalline structure (which is also referred to as 'nanocrystalline structure'), in order to improve the mechanical properties and corrosion resistance of the material, and creating arrays of micro- and nanoparticles (nanoclusters) on its surface, in order to improve its optical, electrical and other properties, e.g., with the aim of enhancing its compatibility with biological tissues. Nanostructures may strongly differ in texture and properties from the bulk material they have been produced on.

Structural details of nanomaterials (grain size, fraction of grain boundaries, structural perfection) have a significant effect on their properties and depend on the preparation procedure [9]. Note that this refers primarily to the mechanical strength of nanomaterials. At a large grain size, the increase in strength and hardness with decreasing grain size is due to the formation of additional grain boundaries, which prevent dislocation motion. It is known that crystallites are dislocation-free when their size is below a certain critical value (for example, iron and nickel particles are dislocation-free when their diameters are below 23 and 140 nm, respectively [73]). Accordingly, the high strength of nanograined materials is due to the low dislocation density and high dislocation formation energy in such materials. The microhardness of nanocrystalline materials is a factor of 2 to 7 higher than that of their coarse-grained analogues [74, 75]. An important point is that they have sufficiently high plasticity [76]. In addition, grain size reduction improves the corrosion resistance and superplasticity of the material.

A key issue in the fabrication of nanocrystalline materials is the ability to ensure a narrow particle size distribution and control over the formation of nanoparticles and process parameters. This can be achieved using laser nanostructuring of materials [5, 8, 9, 77]. The formation of a fine-crystalline or amorphous surface structure under the action of laser pulses is referred to as 'laser glassing' [26, 30, 71, 78].

The first experiments aimed at surface modification of various metals and alloys in order to produce an ultrafine-crystalline or amorphous structure by laser pulses 10^{-9} to 10^{-3} s in duration were performed more than three decades ago and revealed many of the main general trends of laser vitrification (see e.g. Refs [79–82]). Micro- and nanostructured materials were shown to have markedly better physical and, especially, mechanical properties.

First of all, the fabrication of amorphous and nanocrystalline structures by pulsed laser irradiation of metals and various alloys was shown to be conceptually feasible. In particular, using $\sim$ 15-ns ruby laser pulses with an energy density of ~ 3.5 J cm^{-2}, Mazzoldi et al. [80] obtained amorphous layers of the order of 150 nm in thickness on pure Al. The layers contained nanometre-scale ($\sim$ 10 nm) crystalline inclusions. As shown earlier, there is a critical laser cooling rate at which crystallisation can be suppressed to give an amorphous structure. The critical cooling rate depends not only on laser irradiation parameters (laser pulse intensity and duration) but also on properties of the material (thermodynamic characteristics, alloy composition, metal purity and surface condition). The experimentally determined cooling rate needed to completely suppress crystallisation in pure metals illuminated by laser pulses exceeds manyfold the calculated value. The reason for this is that any crystal at the boundary of the irradiated region is a potential seed. In particular, the calculated critical cooling rate for aluminium amorphisation under the conditions of the above experiment is 9.3×10^7 K s^{-1} [72], which is well below the cooling rate used by Mazzoldi et al. [80] (about 10^{10} K s^{-1}).

Several approaches have been proposed for reducing the critical cooling rate for amorphisation. Skakov et al. [81] used additions of so-called glass formers (B, Si, P and C) for this purpose. They irradiated 11 different Fe alloys containing the glass formers. The CO_2 laser output intensity was 10^5 to 10^6 W cm^{-2} and the laser pulse duration was 120 ns. On some of the alloys, they obtained amorphous layers 5 to 10 μm thick. The cooling rate of the alloys containing the glass formers was $\sim 10^6$ K s^{-1}, which is far below the calculated critical cooling rate for amorphisation in pure Fe [72]: $v_{cr} \sim 1.8 \times 10^9$ K s^{-1}.

Matsunawa et al. [82] investigated the formation of a fine-crystalline structure in the $Fe_{78}Si_9B_{13}$ alloy exposed to $\sim$ 0.24-ms Nd:YAG laser pulses. The cooling rate was 1.5×10^5 K s^{-1}. They observed both fine-crystalline and amorphous phases in the surface layer. To further increase the cooling rate, substrates with high thermal conductivity (Ni and Cu) were used as heat sinks. Under such conditions, they obtained amorphous layers on the surface and fine-crystalline layers at the solid–liquid interface. A mixed, ultrafine structure (composed of amorphous and crystalline regions) was also obtained in a mixture of Ni–Nb and Cu–Zr powders exposed to millisecond neodymium glass laser pulses [79]. The cooling rate was 10^5 K s^{-1}. The laser exposure was found to cause the alloys to amorphise in a narrow range of irradiation parameters. Changing the irradiation energy by 10 % to 15 % led to crystallisation of the amorphous material. Fine-crystalline and amorphous structures were observed to form at pulse durations from milliseconds to nanoseconds.

A number of reports analysed the effect of laser pulse duration at different wavelengths on materials processing conditions and compared processing conditions at various laser pulse durations (see e.g. Refs [57, 58, 69]). In particular, Simon and Ihleman [57] irradiated a variety of metals (Ni, Al, Cu, Cr and Au) and semiconductors (Si and Ge) with UV ($\lambda = 248$ nm) laser pulses and compared the morphologies of the irradiated regions at pulse durations of 0.1, 0.5, 5 and 50 ps. They observed the formation of periodic structures with a period of $\sim$ 360 nm and holes less than 1 μm in diameter ($\sim$ 500 nm in copper). At laser pulse durations under 5 ps, the irradiated materials differed very little in morphology, whereas the structures obtained at laser pulse durations from 5 to 50 ps differed markedly. Pulses more than 5 ps in duration produced a melt pool, leading to the formation of solidified droplets on the surface. Moreover, increasing the pulse duration to 50 ps caused the fine periodic structure to blur. In the semiconductors, such structural distinctions were observed even at pulse durations

slightly above 500 fs. When the laser pulse duration was reduced to ~ 200 fs, the ablation process involved the formation of a molten layer. The shape of the solidified melt (the rim of the crater) depended on both the melt flow dynamics and rapid solidification conditions.

Crouch et al. [69] compared the optical properties of microstructures produced on silicon by nanosecond and femtosecond laser pulses. The penguin-like structures produced by 30-ns and 100-fs laser pulses differed in size by a factor of 5: the spikes were 40 and 8 μm in height and 20 and 4 μm in width, respectively. Even though the structures differed markedly in dimensions, morphology and crystallinity, the materials were very similar in optoelectronic properties and chemical composition.

Thus, the morphology and physical properties of layers produced by pulsed laser irradiation are governed not only by the characteristics of the material but also by the laser pulse energy density and duration.

A number of studies were concerned with the effect of femtosecond Ti : sapphire laser pulses ($\lambda = 800$ nm) on the surface morphology of various metals [10, 11, 13, 20, 53, 61, 63]. As shown by Korte et al. [20], structures 100 – 200 nm in size can be produced by the direct action of femtosecond laser pulses using standard photolithographic masks based on Cr-coated layers. Submicron surface structures develop in two cases: (1) below ablation threshold when there is a melt in the affected zone and (2) in the ablation regime when the incident intensity slightly exceeds the ablation threshold owing to careful beam focusing. In this technique, the formation of a nanometre-scale hole on the metal surface is always accompanied by surface distortion of the structure around the hole. Such a structure appears in the region where the incident laser beam intensity exceeds the melting threshold. Various exposure conditions were examined in order to illustrate specific features of the influence of a single laser shot on metals: without redeposition of the ejected material, as well as with redeposition and a solidified ridge around the hole.

Koch et al. [53] studied nanotexturing of gold films at incident laser intensities that ensured melting of the metal in the affected zone. The laser pulse duration was 30 fs, and the incident intensity was just below the ablation threshold but above the melting threshold. For noble metals (e.g. gold), the lifetime of the melt pool was shown to be sufficient for the formation of various surface textures. In particular, conditions were selected for producing 500- to 600-nm bumps with a nanojet of 100 – 200 nm diameter in their central part. The dynamics of the formation of such structures during melting and subsequent solidification are still unclear.

Further attempts to study the morphology of laser-processed gold, copper and titanium surfaces were made by Vorobyev and Guo [10, 11, 61, 63]. In their experiments, the size and shape of surface nanostructures depended not only on the incident laser intensity and number of pulses but also on the properties of the material and the initial structure of the surface. Adjusting the incident intensity and number of pulses, they were able to produce nano-, micro- and macrostructures and various combinations of these on metal surfaces. There were optimal laser processing conditions for each type of structure, in particular for pure surface nanostructuring, i.e., for producing only nanometre-sized surface structures. The nanostructures in the three metals were similar in size and shape. Using 65-fs laser pulses and pulse energy densities just above the damage threshold (the ablation threshold for Au and Ti is 0.067 J cm^{-2} and that for Cu is 0.084 J cm^{-}2), various nanostructures were produced with one to ten laser pulses. These typically had the form of porous structures (round nanopores) 40 – 100 nm in diameter, randomly arranged nanoprotrusions 20 – 70 nm in diameter and 20 – 80 nm in length, nanocraters and various structures (nanorings and elevations) 20 – 100 nm in size around the nanocraters.

Figure 1b shows nanostructures produced on a Cu surface by a single 65-fs laser pulse with an energy density $F = 0.35$ J cm^{-2} [63]. The minimum size of the forming crystalline nanostructure was 20 nm. Studies of the morphology and texture of surface structures demonstrate that nanostructuring is due to randomly arranged nanometre-sized melt pools. The shape and size of the forming nanostructures depend both on the dynamics of melt motion in nanoregions in the zone being irradiated and on the cooling kinetics.

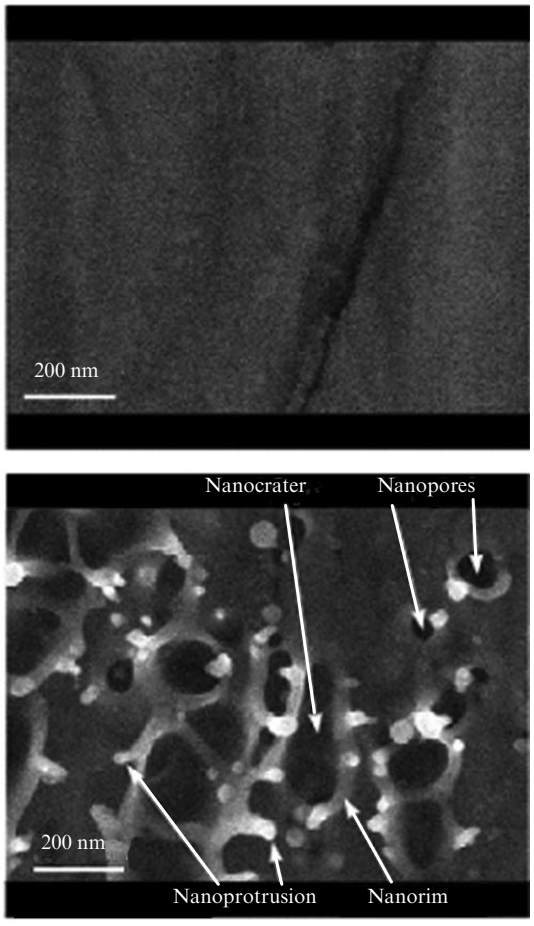

Figure 1. Typical images of (a) a copper surface before irradiation and (b) a nanostructure produced on the copper surface by femtosecond laser ablation (pulse duration, 65 fs; energy density, $F = 0.35$ J cm^{-2}; $N = 1$).

Multiple irradiations can produce ensembles of nanostructures up to 500 nm in size. The process is accompanied by the formation of microstructures, which prevail at a number of pulses $N = 1000$. Similar results can be obtained at higher laser energy densities. Figure 2 presents a scanning electron microscopy (SEM) image of a copper surface after

exposure to two laser pulses with an energy density $F = 9.6$ J cm^{-2} [63]. The central part of the irradiated zone contains only microstructures. At the same time, nanostructures are seen in the peripheral parts of the ablation zone, where the laser energy density is substantially lower. In addition, Vorobyev and Guo [11, 61] observed the formation of periodic structures in gold and titanium at a laser energy density near the ablation threshold and a number of pulses from 20 to 800.

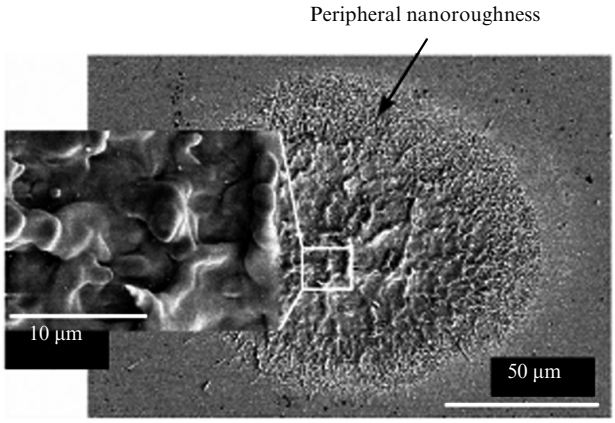

Figure 2. SEM image of a copper surface after exposure to two laser pulses (pulse duration, 65 fs; energy density, $F = 9.6$ J cm^{-2}). Inset: microstructure details in the central part of the irradiated zone.

As pointed out above, the mechanisms underlying the formation of periodic structures at longer pulse durations are well understood [31, 58]. Such structures are sometimes referred to as laser-induced surface periodical structures. Typically, their period is of the order of the incident radiation wavelength and they are oriented perpendicular to the incident wave polarisation. A unique feature of the periodical structures produced by ablation with femtosecond laser pulses in studies by Vorobyev and Guo [11, 61] was that both the elevations and depressions in the periodic microstructures were covered with nanoparticles, predominantly spherical in shape (Fig. 3) [61].

Also of interest is laser ablation at a high energy density and a small number of laser pulses [61], which causes complete melting of the region under irradiation. Subsequent ultrarapid melt solidification leads to the formation of a smooth surface covered with redeposited metal nanoparticles down to ~ 10 nm in size. Figure 4 illustrates the surface topography of titanium after irradiation by femtosecond laser pulses with an energy density of 2.9 J cm^{-2} [61]. Similar structures resulted from picosecond laser irradiation [83], but the number of nanostructures produced by a femtosecond pulse considerably exceeded that in the case of a picosecond pulse.

Note that surface nanostructuring influences the optical properties of metals; in particular, it increases their absorptance. Vorobyev and Guo [11, 63] demonstrated an increase in the absorptance of gold and copper. Selecting an appropriate combination of nano-, micro- and macrostructures on a metal surface, one can increase the absorptance of copper to 85 % and that of gold to 100 %. The ablation crater on gold was shown to be surrounded by a black halo due to spherical aggregates of spherical nanoparticles. Figure 5 shows images of a black gold layer composed of spherical aggregates, whose size decreases with increasing distance from the crater (the crater is situated to the left of the zone in the images) [11]. As seen in Fig. 5b, the spherical redeposited aggregates consist of spherical nanoparticles. Thus, the redeposition of nanoparticles (clusters) outside the beam spot leads to the formation of nanostructured material known as black gold.

Despite the effectiveness of femtosecond laser nanostructuring and nanostructuring with the use of picosecond pulses, there is also practical interest in employing cheaper laser systems generating nanosecond pulses. In particular, Lapshin et al. [68, 84] irradiated various materials by 25-ns F_2 laser pulses of wavelength 157 nm. Their results demonstrate that nanostructures can be produced on solid surfaces by multiple exposures that ensure ablation in the centre of the beam spot and surface melting at its periphery. Figures 6 and 7 present atomic force microscopy (AFM) images illustrating surface nanotopography [68]. Figure 6 shows a nanostructured silicon nitride surface profile after exposure to 500 laser pulses in the melting zone, where the laser energy density was 0.6 J cm^{-2}. The characteristic lateral grain size is 100 – 150 nm, with a height of 100 – 150 nm, and aggregates of small grains are 400 –

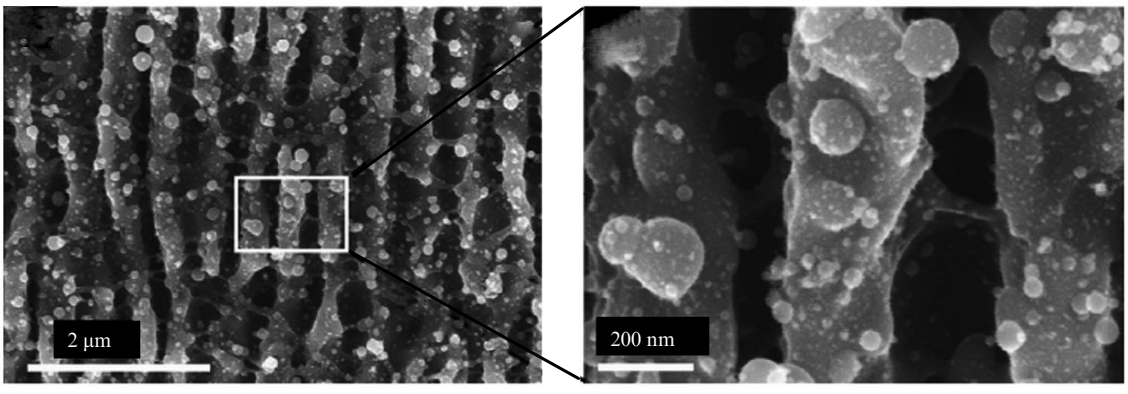

Figure 3. (a) Periodic structure produced on a titanium surface by exposure to femtosecond laser pulses (pulse duration, 65 fs; energy density, $F = 0.067$ J cm^{-2}; $N = 400$); (b) higher magnification image of the area outlined in the left panel, showing details of the periodic structure and nanoparticles.

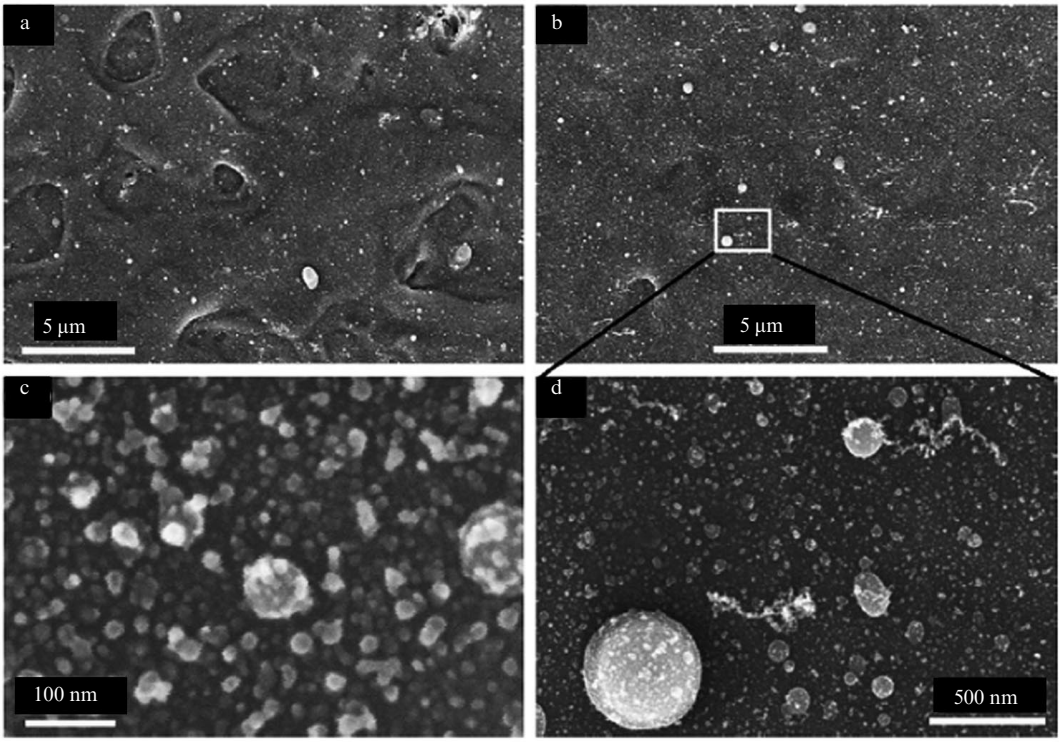

Figure 4. Titanium surface after femtosecond (65 fs, 2.9 J cm^{-2}) laser exposures: (a) smooth surface with microinhomogeneities after exposure to one laser pulse; (b) smooth surface with nanostructures after two laser pulses; (c) higher magnification image of the area outlined in Fig. 4b, showing surface nanostructures; (d) nanotopography of a smooth surface after exposure to four laser pulses (one can see spherical nanostructures down to ~ 10 nm in size.

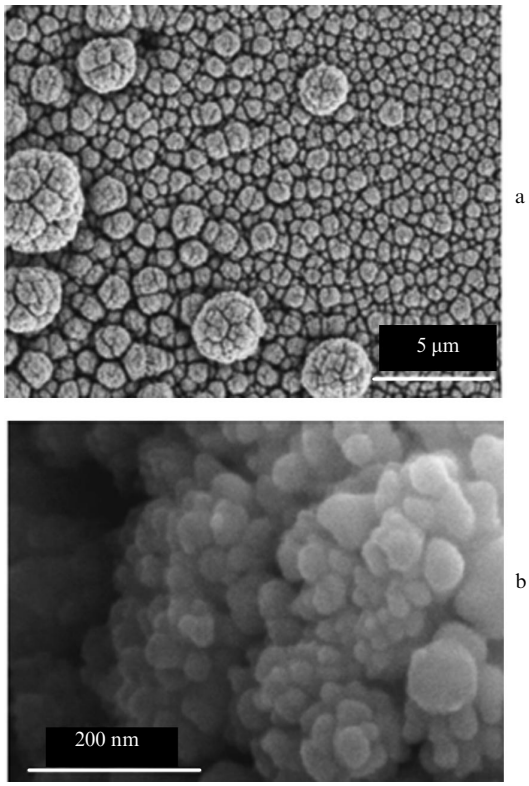

Figure 5. Structure of redeposited black gold outside the beam spot after 20000 laser shots (65 fs, 0.17 J cm^{-2}): (a) black gold layer composed of spherical aggregates; (b) SEM image of spherical nanoparticles that constitute the spherical aggregates in the structure of the black gold.

600 nm in lateral size and ~ 500 nm in height. Note that the unirradiated Si_3N_4 surface ranged in lateral grain size from 60 to 150 nm, but the height of the grains was rather small: 6–20 nm. Near the centre of the beam spot, the energy density was higher, 2 J cm^{-2}. The length scale of the nanostructure in this region was 200 nm to 1.4 μm and the nanoroughness was of the same order.

The surface nanostructuring of diamond-like films is similar to that described above (Fig. 7). An important factor in nanostructuring is inhomogeneity of the surface profile, which may cause inhomogeneity of the ablation process. Ablation first takes place at grain boundaries. After a sufficiently large number of pulses, nanostructuring is determined by laser-induced surface instability. Therefore, optimising the number of laser pulses, one can control the size of the resulting surface nanostructures, in particular, minimise it.

In recent years, diode-pumped solid-state lasers have been used increasingly in technological applications owing to their small dimensions, good beam quality, and high efficiency. They are widely used for the modification and micromachining of semiconductors, ceramics, and metals [24–26]. Pervolaraki et al. [24] reported the use of a $Nd:YVO_4$ laser generating nanosecond (1.7–2.8 ns) pulses of the fundamental (1064 nm) and second (532 nm) harmonics. They studied ablation of polyimide, gold film, and silicon when the melt was ejected from the crater, and analysed conditions for producing high-quality holes in materials.

Bezotosnyi et al. [25] and Zavestovskaya et al. [26] reported extensive experimental studies concerned with the surface modification of metals and semiconductors by

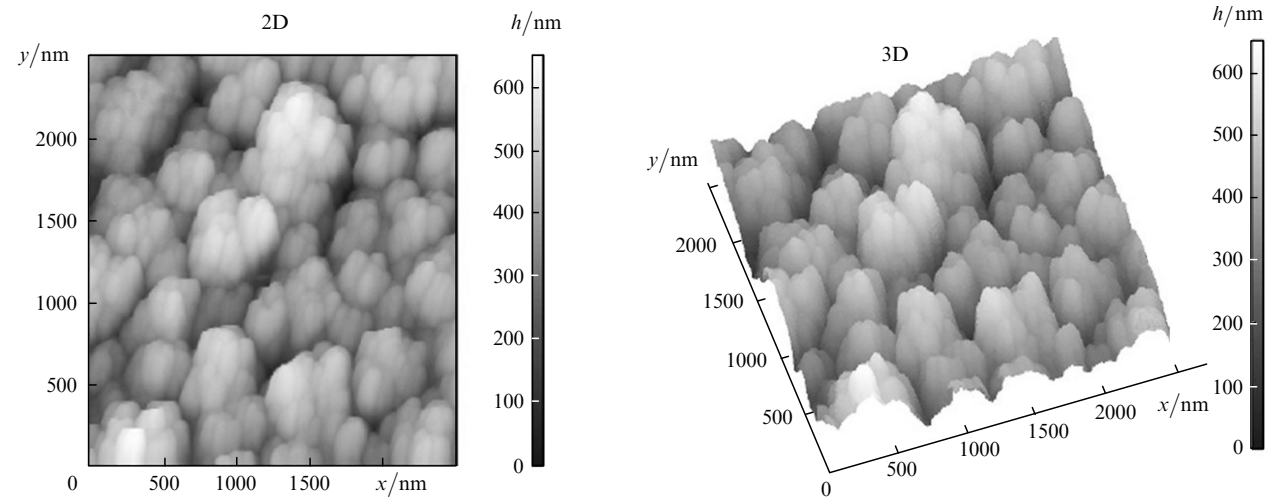

Figure 6. Two- and three-dimensional AFM images of a silicon nitride surface irradiated with 500 laser pulses (25 ns, 0.6 J cm^{-2}).

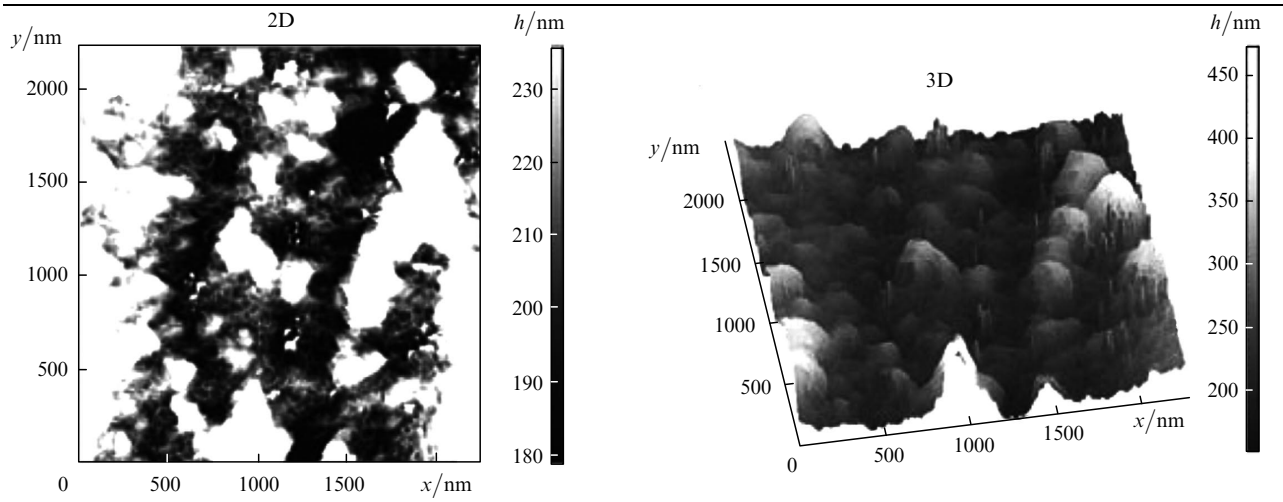

Figure 7. Two- and three-dimensional AFM images of a diamond-like film on a rough copper substrate after 100 laser shots (25 ns, 1.0 J cm−2). One can see cells 60 – 70 nm in characteristic lateral size and 10 – 70 nm in height and widely spaced hillocks 200 – 500 nm in characteristic lateral size and 200 – 300 nm in height.

laser pulses. To this end, they employed a diode-pumped acousto-optically *Q*-switched pulsed Nd : YAG laser [85, 86]. They examined laser modification of indium solder with the aim of improving the effectiveness of heat removal from the crystal of high-power laser diodes [25]. The pulse energy density was 0.1 J cm^{-2}, and the pulse duration was 6.5 ns. The SEM images in Fig. 8 illustrate the effect of laser exposure on the surface morphology of indium solder [25]. The indium film is seen to amorphise (laser glassing). The observed flaws typically ranged in size from 100 nm to 1 μm. Modifying the structure of the solder film immediately before the laser mounting process ensured a marked increase in diode laser output power [25, 26]. Laser-modified indium solders made it possible to reach excellent output parameters of high-power 808-nm laser diodes with good reproducibility.

Thus, the above results on the structure of materials exposed to short and ultrashort laser pulses point to the formation of a fine structure with a grain size in the order of several nanometres. The dimensions and shape of nanostructures depend on the initial surface condition and the number of laser pulses. All types of nanostructures thus produced can be used in technological applications (e.g. to control the optical properties of materials, enhance the compatibility of implants with biological tissues etc.). Laser ablation with femtosecond pulses can be used to manufacture coatings such as black gold films. Direct laser modification of materials surfaces is possible with and without ablation. A necessary condition for modification processes to take place is that there be a melt pool in the zone under irradiation.

Note that the advantages of particular laser processing conditions with a given laser pulse duration depend on the type of material to be processed, laser processing conditions, and processing procedure. All the advantages of direct laser nanomodification of metal surfaces (with no plasma) are a logical (natural) consequence of laser ablation processes. To ensure nanostructuring reproducibility, one should optimise processing parameters such as the heating and cooling time and rate and the volumes of the liquid and crystalline phases. Also important is the ability to determine the average crystallite size. All the above parameters depend

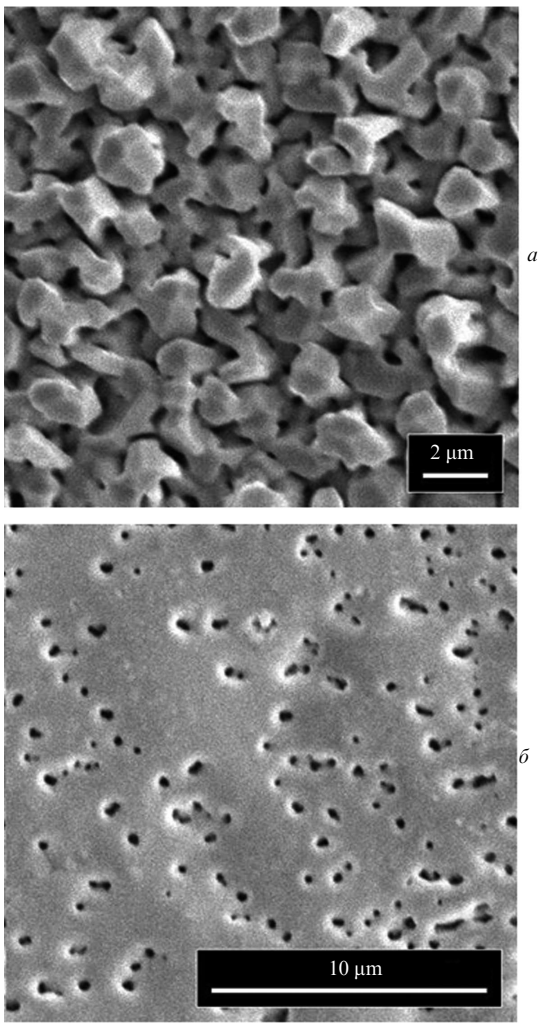

Figure 8. SEM images of a 2.7-μm-thick indium film (a) before and (b) after laser exposure (diode-pumped Nd : YAG laser; pulse duration, 6.5 ns; energy density, 0.1 J cm^{-2}).

on laser pulse parameters and the thermodynamic properties of the material.

3. Theoretical modelling of pulsed-laser-induced nanocrystallisation processes

To construct a model of nanostructuring by short and ultrashort laser pulses, one should study in detail the mechanisms of laser energy absorption, nonequilibrium processes induced by rapid laser energy deposition and structural and phase transformations in laser-processed surface layers of materials. All these processes are closely interrelated. One distinctive feature of these processes is that they may occur within extremely small volumes, down to several hundred microns in size, in just 10^{-13} to 10^{-12} s. As a consequence, there are high heating and cooling rates and large temperature gradients. Laser ablation, or laser-induced material removal (laser etching), has been the subject of extensive theoretical studies [1, 33 – 49, 52]. Melting processes have been analysed in detail for both cw laser radiation and various laser pulse durations (from milli- to femtoseconds) [1, 26, 30, 87 – 92].

An issue that is often addressed in the literature is whether the mechanism of melting induced by ultrashort pulses is thermal or nonthermal [18, 52, 70]. The mechanism of phase transformations is nonthermal when the structural changes involved occur more rapidly than the absorbed energy transfer from electrons to the lattice. The phase transitions that develop after heat transfer from electrons to the lattice are ultrarapid thermal phase transitions.

There is experimental evidence (exemplified by the effect of a femtosecond laser pulse on aluminium) that the mechanism of metal melting by short and ultrashort laser pulses is thermal at pulse durations down to 40 fs [93]. The process is due to lattice heating to the melting point and takes in the order of several picoseconds (1.5 – 2 ps for Al). The new phase nucleates through a homogeneous mechanism. The heating rate may reach 10^{14} K s^{-1}. The time taken by the phase transition is independent of the laser energy density, as distinct from nonthermal melting mechanisms.

Ivanov and Zhigilei [90] reported a computer simulation study of the melting of 50-nm-thick Ni and Au films exposed to laser pulses 200 fs to 150 ps in duration. The simulated melting time was 2 ps. The ablation, melting, and vaporisation of nickel, copper, and quartz were studied using molecular dynamics simulation [91, 92, 94, 95]. It is worth pointing out that the melting and solidification times of materials exposed to femtosecond pulses have been variously reported to be 2 – 20 and 50 – 120 ps, respectively.

The surface structure of a material exposed to a laser pulse is governed by both the melt flow dynamics and solidification kinetics. Fundamental metal solidification processes during ultrarapid cooling have not yet been studied in sufficient detail. This is particularly true of the kinetics and dynamics of the melting and solidification behaviour of metals exposed to ultrashort laser pulses.

The most general approach to describing solidification kinetics during cooling after laser exposure is to examine the distribution of the number of crystalline particles, Z, with respect to the number of atoms per particle, n, at time t [96]. Knowing the distribution function $Z(n, t)$, one can find the mean size of the crystallites formed during cooling and the volume fraction of the new phase. The rate equation for $Z(n, t)$ was treated in a number of studies [71, 72, 97 – 101]. In particular, Kudinov and Shmakov [97] found a solution to a general classic equation for $Z(n, t)$ using an average diffusion coefficient and linearising the rate equation. The solution was used by Tokarev et al. [101] to approximately determine the mean number of particles per crystalline grain and the fraction of melt solidified for a silicon nitride surface exposed to nanosecond F_2 laser pulses.

Zavestovskaya et al. [71, 72] proposed a method for analytically solving the rate equation for the distribution function $Z(n, t)$. The method is based on the operator method that is commonly used to solve the Schrödinger equation. Its salient feature is that it requires no averaging of the diffusion coefficient and builds on the use of specific physical features of metal solidification at ultra-high cooling rates (a large number of supercritical nuclei, absence of very large nuclei and a nearly planar shape of forming crystallites). This allows one to explicitly describe the physical behaviour of kinetic parameters such as the crystallite size and the fraction of crystallised phase as functions of laser exposure parameters.

The distribution function thus derived [72] can be represented in the form

$$Z_f(\alpha,\beta,n) = \frac{\sqrt{n}}{\alpha}\int_0^\infty d\xi Z_{in}\left(\frac{1}{4}\xi^2 e^{\beta}\right) \times \exp\left(-\frac{4n+\xi^2}{4\alpha}\right) I_1\left(\xi\frac{\sqrt{n}}{\alpha}\right), \quad (1)$$

$$\alpha(t) = v\exp[-\beta(t)]\int_0^t \exp\left[\beta(t) - \frac{U}{kT(\tau)}\right]d\tau,$$

$$\beta(t) = -\frac{\Delta h v}{kT_0}\int_0^t \frac{T_0 - T(\tau)}{T(\tau)}\exp\left[-\frac{U}{kT(\tau)}\right]d\tau, \quad (2)$$

where Z_{in} and Z_f are the initial and final distribution functions; I_1 is the first-order modified Bessel function; v is the Debye characteristic frequency; k is the Boltzmann constant; Δh is the latent heat of the phase transition; U is the activation energy for the transfer of an atom across an interface; and T_0 is the solidification temperature. The final forms of $\alpha(t)$ and $\beta(t)$ and, accordingly, the distribution function are determined by the variation of the temperature during cooling, which depends on the laser exposure parameters and the thermophysical properties of the material. Zavestovskaya et al. [72] considered the most typical time dependences of temperature: linear, power-law, and exponential. The $\alpha(t)$ and $\beta(t)$ data obtained for linear cooling are presented in Fig. 9 [71]. It can be seen that, at very high cooling rates, α, β and, accordingly, the distribution function reach a plateau in a small fraction of the total cooling time.

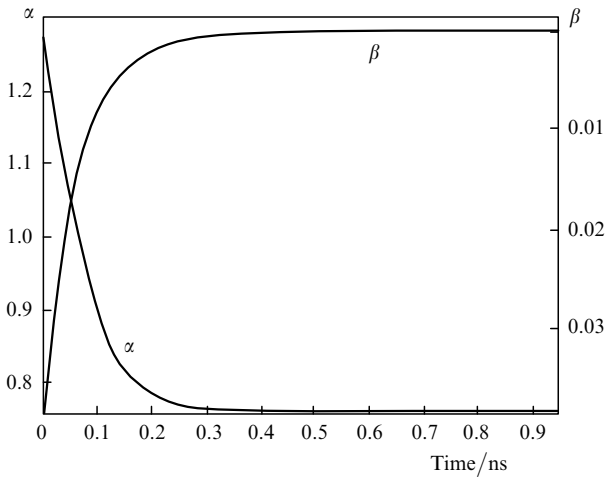

Figure 9. Time dependences of α and β for Fe at a constant cooling rate ($U/kT_0 = 17.1$).

The cooling rate determines the explicit form of the distribution function. For example, with

$$Z_{in} = Z_0\delta(n - n_0), \quad (3)$$

we obtain for linear and power-law cooling

$$Z_f = \left(\frac{n}{\alpha^2}e^{-\beta}\right)^{3/4}\exp\left[-\frac{(\sqrt{n} - \sqrt{n_0}e^{-\beta/2})}{\alpha}\right]. \quad (4)$$

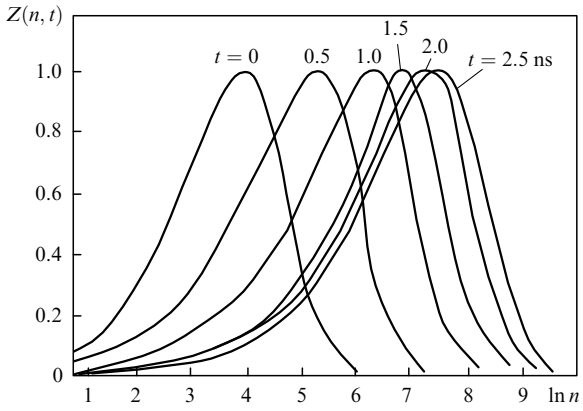

Figure 10. Distribution function $Z(n, t)$ between times $t = 0$ and 2.5 ns ($U/kT_0 = 15$).

Figure 10 illustrates the time variation of $Z(n, t)$ [71]. It is seen that, in the initial stage of cooling, the function shifts (drifts) significantly, whereas at the end of cooling it remains essentially unchanged.

Using (4), the relative change in the volume of the forming phase can be represented in the form [71]

$$\frac{\Delta V}{V} = \frac{V_{in} - V_f}{V_{in}} = \frac{N\Delta V - Ne^{\beta}\Delta V}{N\Delta V} = 1 - e^{\beta}, \quad (5)$$

where N is the number of laser pulses. Another important parameter is the average size of the crystalline nuclei of the forming phase, or the average number of atoms per nucleus [71]:

$$\frac{\Delta V}{V} = \frac{V_{in} - V_f}{V_{in}} = \frac{N\Delta V - Ne^{\beta}\Delta V}{N\Delta V} = 1 - e^{\beta}. \quad (5)$$

Note that $\langle n\rangle$ is completely determined by α, i.e., by the broadening of the distribution, and that the $\Delta V/V$ ratio depends only on β, i.e., on the drift of the distribution function with an increase in the number of particles.

Figure 11 presents the calculated volume of the crystallised melt as a function of cooling rate and thermodynamic properties of the material for exponential cooling. It can be seen that, at relatively slow cooling rates ($\exp\beta \to 0$), the melt crystallises almost completely ($\Delta V/V \to 1$). The corresponding cooling rates are 1.8×10^6 K s^{-1} for Fe, 2.8×10^5 K s^{-1} for Al and 1.73×10^5 K s^{-1} for Ni. With increasing cooling rate, only part of the melt crystallises. In the $t \to \infty$ limit, we have $\exp\beta \to 1$ и $\Delta V/V \to 0$. It is then reasonable to assume that the rest of the melt tends to form a noncrystalline, amorphous phase (a solidified liquid). In particular, we find in the case of Fe that, even at cooling rates approaching $v_{cr} = 1.8 \times 10^9$ K s^{-1}, approximately 0.996 of the melt may have the form of a solidified liquid. Amorphous phases of Al and Ni may form at $v_{cr} \approx 9.3 \times 10^8$ and 7.3×10^7 K s^{-1}, respectively.

Note that the condition $v \geqslant v_{cr}$ is a kinetic criterion for amorphisation. Zavestovskaya et al. [72] established an amorphisation criterion from the condition that an amorphous phase is formed when its volume fraction approaches a value, P, close to unity. The experimentally observed

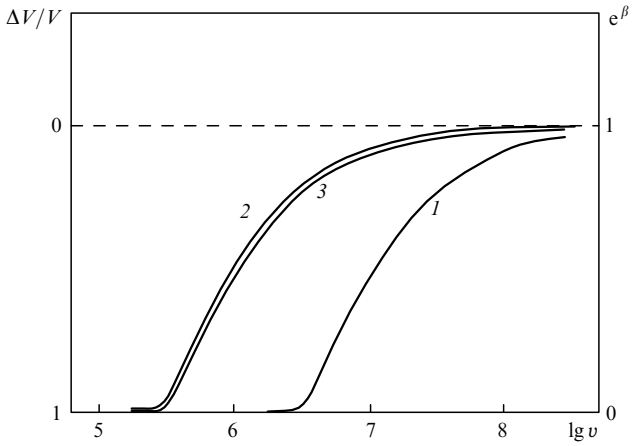

Figure 11. Semilog plots of the volume fraction of crystallised phase vs. cooling rate for (*1*) Fe, (*2*) Al and (*3*) Ni.

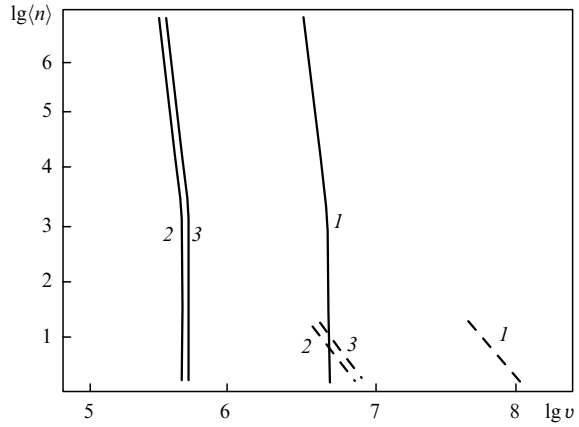

Figure 12. Log–log plots of the average number of atoms per crystallite, $\langle n \rangle$, against cooling rate for (*1*) Fe, (*2*) Al and (*3*) Ni.

crystalline content is $\sim 10^{-6}$ [102]; therefore, $\exp[\beta(t \to \infty)] = P$.

On the other hand, the rate of heat transfer from the melt to the material during solidification is determined by its thermophysical properties and sets the upper limit of the cooling rate. In the case of pulsed laser exposure, the cooling rate has a maximum near the solidification temperature [30]:

$$v_{\max} = Aq \Big/ \left(\lambda_{\mathrm{m}} \sqrt{\frac{\varkappa}{\pi\tau}} \right), \tag{7}$$

where A is an effective absorptance; $\varkappa$ is the thermal diffusivity; λ_{m} is the thermal conductivity of the material; q is the incident intensity; and τ is the laser pulse duration. Relation (7) was used to determine the critical cooling rate at which a noncrystalline (amorphous) phase can be obtained for $U/kT_0 > 5$ [72]:

$$_{\mathrm{cr}} = \frac{v\Delta h(1-c_0)}{U \ln P} \exp\left(-\frac{U}{kT_0}\right), \tag{8}$$

where c_0 is constant at ~ 0.95. It can be seen that whether an amorphous phase can be obtained depends on both the laser pulse parameters and the thermodynamic properties of the material.

Note that Eqn (8) for the cooling rate needs to be refined when thin layers of a material are processed and the cooling rate depends significantly on the thickness of the melt pool [84].

Figure 12 shows log–log plots of the average number of atoms per crystallite, $\langle n \rangle$, against cooling rate [71]. Even a slight decrease in cooling rate is seen to lead to a sharp drop (by several orders of magnitude) in $\langle n \rangle$.

When metals are irradiated by pulses of a diode-pumped solid-state laser, the cooling rate is such that structures 100 to 400 nm in size may form on an indium surface. When femtosecond laser pulses are used, the crystallite size is 20–40 nm, in good agreement with experimental data [10, 11].

Detailed calculations, including numerical modelling, and a quantitative comparison with experimental data are hindered by the lack of accurate thermodynamic data for the system. Moreover, when femtosecond laser pulses are used the cooling rate of materials may reach 10^{12} K s^{-1}, and the structure of the solidified melt and the presence, shape and size of nanostructures may be governed by the dynamics of the processes that occur in the melt during cooling [63].

4. Conclusions

Research into the processes underlying surface micro- and nanostructuring of metals and other materials by short and ultrashort laser pulses has been reviewed, with focus on direct laser irradiation involving melting of the material (with or without ablation), followed by ultrarapid surface solidification after the laser pulse. Experimental data for nano-, pico- and femtosecond laser pulses demonstrate the possibility of producing structures with dimensions in the nanometre range and the possibility of amorphisation. All the types of nanostructures thus produced can be used in a number of technological applications (e.g. to control the mechanical and optical properties of metals and other materials, enhance the compatibility of implants with biological tissues etc.).

The results of theoretical studies of the solidification kinetics of molten metals have been analysed for ultra-high cooling rates in materials processing with ultrashort laser pulses. An analytical solution to the rate equation for the crystallite size distribution after ultrarapid cooling has been used to evaluate the average number of atoms per crystallite and the size of crystalline grains resulting from pulsed laser irradiation of metal surfaces. Determination of the volume fraction of crystallised phase allows one to find the critical cooling rate at which crystallisation is impossible and the structure amorphises.

The data presented in this study can be used to optimise direct laser micro- and nanostructuring conditions and to ensure process control and reproducibility.

Acknowledgements. I gratefully thank O.N. Krokhin for his encouraging interest in this work; Yu.M. Popov and A.P. Kanavin for helpful discussions; V.V. Bezotosnyi, A.Yu. Vorobyev, A.V. Kabashin, V.N. Tokarev, E.A. Cheshev and B.N. Chichkov for informing me of their results;

and N.A. Kozlovskaya for her assistance in preparing the manuscript.

This work was supported by the Russian Academy of Sciences (Programme Nos 21P and 7OF), the Russian Foundation for Basic Research (Grant No. 09-02-00615) and the RF Ministry of Education and Science (Grant No. 2009-1.1-122-052-025).

References

1. Anan'in O.B., Afanasiev Yu.V., Bykovskii Yu.A., Krokhin O.N. *Lazernaya plazma. Fizika i primeneniya* (Laser Plasma: Physics and Applications) (Moscow: Mosk. Inzhenerno-Fizicheskii Inst., 2003) p. 400.
2. Prasad P.N. *Introduction to Biophotonics* (Boston: Wiley-Interscience, 2003).
3. Kabashin A.V., Meunier M., in *Recent Advances in Laser Processing of Materials* (Amsterdam: Elsevier, 2006) p. 1.
4. Bauerle D., Pedarnig J.D., Vrejoiu I., Peruzzi M., Matei D.G., Brodoceanu D., Dinescu M. *Rom. Rep. Phys.*, **57** (4), 935 (2005).
5. Arnold B.G., Pique A. *MRS Bull.*, **32**, 9 (2007).
6. Ganatios S., Badita L.-L., Beca P. *Rom. Rev. Precis. Mech., Opt. Mechatronics*, **18** (34), 129 (2008).
7. Kabashin A.V., Delaporte Ph., Pereira A., Grojo D., Torres R., Sarnet Th., Sentis M. *Nanoscale Res. Lett.*, **5**, 454 (2010).
8. Gamaly E.G., Rode A.V. *Encyclopedia of Nanoscience and Nanotechnology*, **10**, 1 (2004).
9. Lyakishev N.P., Alymov M.I. *Ross. Nanotekhnol.*, **1** (1-2), 71 (2006).
10. Vorobyev A.Y., Guo C. *J. Phys.: Conf. Ser.*, **59**, 579 (2007).
11. Vorobyev A.Y., Guo C. *Phys. Rev. B*, **72**, 195422 (2005).
12. Zavedeev E.V., Petrovskaya A.V., Simakin A.V., Shafeev G.A. *Kvantovaya Elektron.*, **36** (10), 978 (2006) [*Quantum Electron.*, **36** (10), 978 (2006)].
13. Vorobyev A.Y., Guo C. *Appl. Phys. Lett.*, **92**, 041914 (2008).
14. Stratakis E., Zobra V., Barberoglou M., Fotakis C., Shafeev G.A. *Appl. Surf. Sci.*, **255**, 5346 (2009).
15. Stratakis E., Zobra V., Barberoglou M., Fotakis C., Shafeev G.A. *Nanotechnology*, **20**, 105303 (2009).
16. Halbwax M., Sarnet T., Delaporte Ph., Sentis M., Etienne H., Torregrossa F., Vervisch V., Perichaud I., Martinuzzi S. *Thin Solid Films*, **516**, 6791 (2008).
17. Denisyuk A.I., in *Problemy kogerentnoi i nelineinoi optiki* (Topics in Coherent and Nonlinear Optics) (St. Petersburg: SpbGU ITMO, 2008) p. 52.
18. Nolte S., Chichkov B.N., Welling H., Shani Y., Lieberman K., Terkel H. *Opt. Lett.*, **24** (13), 914 (1999).
19. Eliseev P.G., Sun H.-B., Juodkazis S., Sugahara T., Sakai S., Misawa H. *Jpn. J. Appl. Phys.*, **38**, 839 (1999).
20. Korte F., Serbin J., Koch J., Erbert A., Fallnich C., Ostendorf A., Chichkov B.N. *Appl. Phys. A*, **77**, 229 (2003).
21. Weisbuch F., Tokarev V.N., Lazare S., Belin C., Bruneel J.L. *Thin Solid Films*, **453-454**, 394 (2004).
22. Barcikowski S., Hahn A., Kabashin A.V., Chichkov B.N. *Appl. Phys. A*, **87**, 47 (2007).
23. Kryukov P.G. *Femtosekundnye impul'sy. Vvedenie v novuyu oblast' lazernoi fiziki* (Femtosecond Pulses: Introduction to a Novel Area of Laser Physics) (Moscow: Fizmatlit, 2008).
24. Pervolaraki M., Dyer P.E., Monk P. *Appl. Phys. A*, **79**, 849 (2004).
25. Bezotosnyi V.V., Bondarev V.Yu., Kovalenko V.I., Krokhin O.N., Pevtsov V.F., Popov Yu.M., Tokarev Yu.N., Cheshev E.A. *Kvantovaya Elektron.*, **37** (11), 1055 (2007) [*Quantum Electron.*, **37** (11), 1055 (2007)].
26. Zavestovskaya I.N., Bezotosnyi V.V., Kanavin A.P., Kozlovskaya N.A., Krokhin O.N., Oleshchenko V.A., Popov Yu.M., Cheshev E.A. *Trudy II Simpoziuma po kogerentnomu opticheskomu izluchheniyu poluprovodnikovykh soedinenii i struktur* (Proc. II Symp. on Coherent Optical Radiation from Semiconductor Materials and Structures) (Moscow: RIIS FIAN, 2010) p. 165.
27. Anisimov S.I., Luk'yanchuk B.S. *Usp. Fiz. Nauk*, **172**, 301 (20002).
28. Anisimov S.I., Imas Ya.A., Romanov G.S., Khodyko Yu.V. *Deistvie izlucheniya bol'shoi moshchnosti na metally* (Effect of High-Power Radiation on Metals) (Moscow: Nauka, 1970).
29. Ready J.F. *Effect of High Power Laser Radiation* (New York: Acad. Press, 1971).
30. Rykalin N., Uglov A., Zuev I., Kokora A. *Lazernaya i elektronno-luchhevaya obrabotka materialov* (Electron-Beam and Laser Processing of Materials) (Moscow: Mir, 1988).
31. Prokhorov A.M., Konov V.I., Ursu I., Mihailesku I.N. *Laser Heating of Metals* (Bristol: Hilger, 1990).
32. Koroteev N.I., Shumai I.L. *Fizika moshchnogo lazernogo izlucheniya* (Physics of High-Power Laser Radiation) (Moscow: Nauka, 1991).
33. Basov N.G., Krokhin O.N. *Zh. Eksp. Teor. Fiz.*, **46**, 171 (1964).
34. Afanasiev Yu.V., Krokhin O.N. *Zh. Eksp. Teor. Fiz.*, **52**, 966 (1967).
35. Afanasiev Yu.V., Krokhin O.N. *Tr. Fiz. Inst. im. P.N. Lebedeva, Akad. Nauk SSSR*, **52**, 118 (1970).
36. Afanasiev Yu.V., Krokhin O.N., in *Fizika vysokikh plotnostei energii* (Physics of High Energy Densities) (Moscow: Mir, 1974).
37. Kanavin A.P., Smetanin I.V., Afanasiev Yu.V., Chichkov B.N., Isakov V.A. *Phys. Rev. B*, **57**, 14698 (1998).
38. Afanasiev Yu.V., Chichkov B.N., Demchenko N.N., Isakov V.A., Zavestovskaya I.N. *J. Russ. Laser Res.*, **20** (2), 89 (1999).
39. Afanasiev Yu.V., Chichkov B.N., Isakov V.A., Kanavin A.P., Uryupin S.A. *J. Russ. Laser Res.*, **20** (3), 189 (1999).
40. Afanasiev Yu.V., Chichkov B.N., Demchenko N.N., Isakov V.A., Zavestovskaya I.N. *J. Russ. Laser Res.*, **20** (6), 489 (1999).
41. Afanasiev Yu.V., Isakov V.A., Zavestovskaya I.N., Chichkov B.N., Von Alvensleben F., Welling H. *Laser Part. Beams*, **17** (4), 585 (1999).
42. Afanasiev Yu.V., Chichkov B.N., Isakov V.A., Kanavin A.P., Uryupin S.A. *J. Russ. Laser Res.*, **21** (6), 505 (2000).
43. Afanasiev Yu.V., Demchenko N.N., Zavestovskaya I.N., Isakov V.A., Kanavin A.P., Uryupin S.A., Chichkov B.N. *Izv. Akad. Nauk*, **63** (4), 667 (1999).
44. Il'inskii Yu.A., Keldysh L.V. *Electromagnetic Response of Material Media* (New York: Plenum Press, 1994).
45. Gamaly E.G., Rode A.V., Luther-Davies B., Tikhonchuk V.T. *Phys. Plasmas*, **9** (3), 949 (2002).
46. Zavestovskaya I.N., Eliseev P.G., Krokhin O.N. *Appl. Surf. Sci.*, **248**, 313 (2005).

47. Zavestovskaya I.N., Eliseev P.G., Krokhin O.N., Men'kova N.A. *Appl. Phys. A*, **92**, 903 (2008).
48. Kanavin A.P., Uryupin S.A. *Phys. Lett. A*, **372**, 2069 (2008).
49. Kanavin A.P., Uryupin S.A. *Kvantovaya Elektron.*, **38** (2), 159 (2008) [*Quantum Electron.,* **38** (2), 159 (2008)].
50. Basov N.G., Bertyaev B.I., Zavestovskaya I.N., Igoshin V.I., Katulin V.A. *'Primenenie lazerov v narodnom khozyaistve'. Trudy vses. konf.* (Proc. All-Union Conf. Application of Lasers in the National Economy) (Moscow: Nauka, 1985) p. 100.
51. Zavestovskaya I.N., Igoshin V.I., Shishkovskii I.V. *Kvantovaya Elektron.*, **16** (8), 1636 (1989) [*Sov. J. Quantum Electron.*, **19** (8), 1053 (1989)].
52. Uteza O.P., Gamaly E.G., Rode A.V., Samoc M., Luter-Davies B. *Phys. Rev. B*, **70**, 054108 (2004).
53. Koch J., Korte F., Bauer T., Fallnich C., Ostendorf A., Chichkov B.N. *Appl. Phys. A*, **81**, 325 (2005).
54. Veiko V.P., Kieu Q.K. *Kvantovaya Elektron.*, **37** (1), 92 (2007) [*Quantum Electron.*, **37** (1), 92 (2007)].
55. Komlenok M.S., Pimenov S.M., Kononenko V.V., Konov V.I., Scheibe H.-J. *J. Nano Microsyst. Technol.*, **3**, 48 (2008).
56. Zavestovskaya I.N. *Laser Part. Beams*, **28**, 437 (2010).
57. Simon P., Ihleman J. *Appl. Surf. Sci.*, **109/110**, 25 (1997).
58. Kononenko T.V., Garnov S.V., Pimenov S.M., Konov V.I., Romano V., Borsos B., Weber H.P. *Appl. Phys. A*, **71**, 627 (2000).
59. Bonze J., Sturm H., Schmidt D., Kautek W. *Appl. Phys. A*, **71**, 657 (2000).
60. Costache F., Henik M., Reif J. *Appl. Surf. Sci.*, **186**, 352 (2002).
61. Vorobyev A.Y., Guo C. *Appl. Surf. Sci.*, **253**, 7272 (2007).
62. Bulgakov A.V., Ozerov I., Marine W. *Thin Solid Films*, **453-454**, 557 (2004).
63. Vorobyev A.Y., Guo C. *Opt. Express*, **14** (6), 2164 (2006).
64. Kabashin A.V., Trudeau A., Marine W., Meunier M. *Appl. Phys. Lett.*, **91**, 201101 (2007).
65. Sanz M., De Nalda R., Marco J.F., Izquierdo J.G., Banares L., Castillejo M. *J. Phys. Chem. C*, **114**, 4864 (2010).
66. Dolgaev S.I., Simakin A.V., Voronov V.V., Shafeev G.A. Bozon-Verduraz F. *Appl. Surf. Sci.*, **186**, 546 (2002).
67. Anikin K.V., Melnik N.N., Simakin A.V., Shafeev G.A., Voronov V.V., Vitukhnovsky A.G. *Chem. Phys. Lett.,* **366**, 357 (2002).
68. Lapshin K.E., Obidin A.Z., Tokarev V.N., Khomich V.Yu., Shmmakov V.A., Yamshchikov V.A. *Ross. Nanotekhnol.*, **2** (11-12), 50 (2007).
69. Crouch C.H., Carey J.E., Warr5nder J.M., Aziz M.J., Mazur E., Genin F.Y. *Appl. Phys. Lett.*, **84** (11), 1850 (2004).
70. Hertel I.V., Stoian R., Rosenfeld A., Ashkenasi D., Campbell E.E.B. *RIKEN Rev.*, **32**, 23 (2001).
71. Zavestovskaya I.N., Kanavin A.P., Men'kova N.A. *Opt. Zh.*, **75** (6), 13 (2008).
72. Zavestovskaya I.N., Igoshin V.I., Kanavin A.P., Shishkovskii I.V. *Tr. Fiz. Inst. im. P.N. Lebedeva, Akad. Nauk SSSR*, **217**, 3 (1993).
73. Gryaznov V.G., Kaprelov A.M., Romanov A.E. *Pis'ma Zh. Tekh. Fiz.*, **15** (2), 39 (1989).
74. Siegel R.W., Fougere G.E. *Nanostruct. Mater.*, **6** (1-4), 205 (1995).
75. Kaibyshev O.A., Utyashev F.Z. *Sverkhplastichnost', izmel'chenie struktury i obrabotka trudnodeformiruemykh splavov* (Superplasticity, Structure Refinement and Processing of Difficult to Deform Alloys) (Moscow: Nauka, 2002).
76. Ovid'ko E., Gutkin E. *Fizicheskaya mekhanika deformiruemykh nanostruktur* (Physical Mechanics of Deformable Nanostructures), Vol. 1: Nanokriistallicheskie materialy (Nanocrystalline Materials) (St. Petersburg: Yanus, 2003).
77. Vladislavlev A.A., Alisin V.V., Roshchin M.N. *'Nanotekhnologii i ikh vliyanie na trenie, iznos i ustalost' v mashinakh'. Trudy mezhdunar. konf.* (Proc. Int. Conf. Nanotechnologies and Their Influence on Friction, Wear and Fatigue in Machines) (Moscow: IMASh, 2004) p. 11.
78. Il'in A.I., Kraposhin V.S. *Poverkhnost*, **6**, 5 (1983).
79. Kashkin V.M., Zhdanov G.S., Mirkin L.I. *Dokl. Akad. Nauk SSSR*, **249**, 1118 (1979).
80. Mazzoldi P., Della Mea G., Battaglin G., Miotello A., Servidori M., Bacci D., Jannitti E. *Phys. Rev. Lett.*, **44**, 88 (1980).
81. Skakov Yu.A., Enderal N.V., Mazorra Kh.A., Kraposhin V.S. *Tr. Mosk. Inst. Stali Splavov*, **147**, 8 (1983).
82. Matsunawa A., Katayama S., Ohmi Y., Kuroki T., in *Proc. LAMP'87* (Osaka: High Temperature Society of Japan, 1987) p. 7.
83. Trtica M., Garovic B., Batani D., Desai T., Panjan P., Radak B. *Appl. Surf. Sci.*, **253**, 2551 (2006).
84. Lapshin K.E., Obidin K.Z., Tokarev V.N., Khomich V.Yu., Shmakov V.A., Yamshchikov V.A. *Fiz. Khim. Obrab. Mater.*, **1**, 43 (2008).
85. Bezotosnyi V.V., Glushchenko N.F., Zalevskii I.D., Popov Yu.M., Semenkov Yu.P., Cheshev E.A. *Kvantovaya Elektron.*, **35** (6), 507 (2005) [*Quantum Electron.*, **35** (6), 507 (2005)].
86. Bezotosnyi V.V., Cheshev E.A., Gorbunkov M.V., Kostrykov P.V., Tunkin V.G. *Appl. Opt.*, **47** (24), 1 (2008).
87. Hsu S.C., Chakravorty S., Mehrabian R. *Metall. Trans. B*, **9**, 221 (1978).
88. Afanasiev Y.V., Zavestovskaya I.N., Kanavin A.P., Kayukov S.V., in *Laser Interaction and Related Plasma Phenomena* (New York: AIP Press, 1995) p. 1274.
89. Tokarev V.N., Kaplan A.F.N. *J. Appl. Phys.*, **86** (5), 2836 (1999).
90. Ivanov D.S., Zhigilei L.V. *Phys. Rev. B*, **68**, 064114 (2003).
91. Xu X., Cheng C., Chowdhury I.H. *J. Heat Transfer*, **126**, 727 (2004).
92. Cheng C., Xu X. *Phys. Rev B*, **72**, 165415 (2005).
93. Kandyla M., Shih T., Mazur E. *Phys. Rev. B*, **75**, 214107 (2007).
94. Cheng C., Xu X. *Intern. J. Thermophys.*, **28** (1), 9 (2007).
95. Cheng C., Wu A.Q., Xu X. *J. Phys.: Conf. Ser.*, **59**, 100 (2007).
96. Christian J.W. *The Theory of Transformations in Metals and Alloys. Part I* (Oxford: Pergamon Press, 1975).
97. Kudinov G.M., Shmakov V.A. *Dokl. Akad. Nauk SSSR*, **264** (6), 610 (1982).
98. Shklovskii V.A., Motornaya A.A., Maslov K.V. *Poverkhnost*, **6**, 91 (1983).
99. Vil'kovskii S.S., Naberezhnykh V.P., Selyakov B.I., in *Nauchnye trudy MISIS 'Amorfnye metallicheskie splavy'* (Amorphous Metallic Alloys: Scientific Works, Moscow Institute of Steel and Alloys) (Moscow: Metallurgiya, 1983) p. 14.

100. Glytenko A.L., Shmakov V.A. *Dokl. Akad. Nauk SSSR*, **276** (6), 1392 (1984).
101. Tokarev V.N., Khomich V.Yu., Shmakov V.A., Yamshchikov V.A. *Dokl. Akad. Nauk*, **419** (6), 1 (2008).
102. Miroshnichenko I.S. *Zakalka iz zhidkogo sostoyaniya* (Quenching from the Liquid State) (Moscow: Metallurgiya, 1982).